JOURNAL OF APPLIED ELECTROCHEMISTRY 18 (1988) 745–750

Investigation of tellurium electrocrystallization by EHD impedance technique

C. DESLOUIS, G. MAURIN, N. PEBERE[1], B. TRIBOLLET

LP 15 du CNRS "Physique des Liquides et Electrochimie", Tour 22, 4 place Jussieu, 75252 Paris Cédex 05, France

[1]*UA 445 du CNRS "Laboratoire de Métallurgie Physique", ENS Chimie, 31077 Toulouse Cédex, France*

Received 20 January 1988; revised 18 March 1988

Electrohydrodynamical impedance measurements were performed during tellurium electrodeposition and correlated to the morphology of the deposits as observed by SEM. In particular, when the current is under a pure mass transport control, microdendrites are formed with various shapes depending on experimental conditions. EHD diagrams are then characteristic of a non-uniformly accessible surface. The calculated dimensions of active zones are in agreement with the sizes of the observed dendrite bushes.

1. Introduction

Tellurium is a constituent common to several definite compounds having semiconducting properties which can be obtained by electrolytic deposition (e.g. CdTe, ZnTe, $CdTe_xSe_{1-x}$, etc.). The low solubility of tellurium oxide in acidic aqueous solution explains why its kinetics of electrodeposition, in the binary or tertiary alloys [1, 2] involved, is mainly controlled by mass transport. As a consequence, mass transport by diffusion and convection is often the rate determining step of the overall kinetics. For this reason, we began a study of the electrodeposition of tellurium alone by focussing our interest on the influence of hydrodynamic conditions. The technique based on a flow modulation (or EHD impedance method [3, 4]), which allows a frequency analysis in mass transport controlled conditions, was therefore used.

Early studies on tellurium electrodeposition connected with Cd/Te electrodeposition evidenced, in some cases, a dendritic growth as can be expected for a system under complete mass transport control and fast interfacial kinetics [5]. Such a geometry could be analyzed in terms of a space-distributed reactivity where the active area is restricted to the tips of the outgrowths and may therefore be considered as a plane electrode consisting of active and passive sites randomly spread over the electrode surface.

In this respect, the EHD impedance response on a planar system with a periodically distributed reactivity has recently been theoretically predicted and experimentally verified [6]. For practical applications, a criterion for determining the space period dimension – or more generally the average dimension of the elementary active sites – was established.

The major aim of this work was to attempt a correlation between the kinetic information provided by the EHD impedance technique and the morphological features of the interface observed by scanning electron microscopy (SEM).

2. Experimental details

Tellurium was deposited under the same conditions as those used for cadmium telluride, i.e. from an aqueous solution of 0.2 M K_2SO_4 saturated with TeO_2. The pH was adjusted to 2.2 and the temperature maintained at 85° C. The concentration of soluble $HTeO_2^+$ species was estimated to 4×10^{-4} M according to Lyons *et al.* [7]. The cathode was a rotating disc (Ti or Ni) 12 mm diameter, carefully polished before each experiment. EHD impedance measurements were performed by means of a FRA Solartron 1170 with conventional potentiostatic regulation. The mechanical set-up, the motor and servo-system necessary for achieving EHD measurements were described in detail in [8]. In parallel, scanning microscopy photographies were taken just after each EHD experiment and compared with the relevant impedance diagrams.

3. Results

3.1. *D.c. measurements*

A predeposition was performed for a few minutes at −0.7 V (SSE) so as to ensure a full coverage of the substrate and then the cathodic polarization curves were recorded in quasi-steady state conditions, starting from −0.4 V (SSE). A plateau current was observed in the potential range between about −0.7 and −1 V (SSE) (Fig. 1).

This current plotted as a function of $\bar{\Omega}^{1/2}$ deviates slightly from a straight line. A straight line is obtained by plotting the reciprocal current as a function of $\bar{\Omega}^{-1/2}$, as shown in Fig. 2. However, a small but discernible positive intercept, I_∞^{-1}, with the ordinate axis is observed. The physical meaning of this effect is generally ascribed to the existence of a process coupled in series with mass transport [9], as explained for CdTe [10, 11]. This can also be due to a non-uniform reactivity of the interface with an inactive fraction of the

0021-891X/88 $03.00 + .12

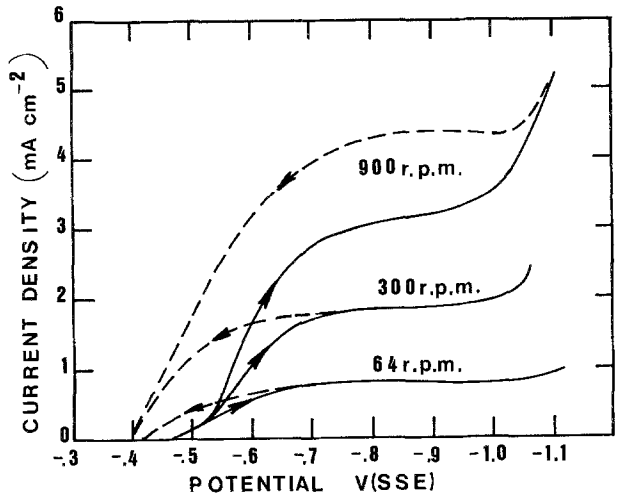

Fig. 1. Current–potential curves of tellurium electrodeposition on a titanium rotating disc electrode. Electrolyte: saturated TeO_2 in 0.2 M K_2SO_4 solution, pH 2.2, θ = 85°C. (Dotted curves are obtained after the formation of microdendrites at −1.1 V (SSE).)

total area which should remain small, in the present case, due to the low value of I_∞^{-1} [6]. This plateau current, I_d, is thus clearly due to mass transport by convective diffusion, as confirmed further by EHD impedance measurements. I_d changes slightly with time, but was considered as constant within each experiment. However, morphological changes were observed in parallel and two regimes can be identified.

(i) At low rotation speeds ($\bar{\Omega}$ < 600 rpm) when the potential is set in the mixed kinetics domain (i.e. $I < I_d$) according to the previously defined procedure the deposit is smooth and the current stable (solid line curve in Fig. 1). On the diffusion plateau, a dendritic growth is observed. Nevertheless, the current remains constant because the size of the dendrites is smaller than the diffusion layer thickness δ. Starting from this last condition, if the cathodic potential is decreased to reach back to the mixed kinetic domain the current now has higher values (dashed curves for Ω = 64 or 300 rpm in Fig. 1) than previously. The potential being kept constant, the current slowly decays to reach a value located on the solid line curve.

The higher values of the dashed curves are explained by the fact that in this potential range the kinetic control is primarily due to charge transfer so that the current is proportional to the developed area (increased by the previous dendritic growth) rather than to the geometrical area in the pure diffusion controlled conditions.

(ii) At high rotation speeds ($\bar{\Omega}$ > 600 rpm) the plateau current is still quite stable if the cathodic potential is maintained below ≈0.9 V (SSE). But if it is set beyond ≈1.0 V (SSE), a sharp increase of the current is observed, related to the growth of large fern-like dendrites. This sudden structural change is clearly correlated to hydrogen evolution reaction. If the potential is now set again in the diffusion plateau domain, the current is substantially higher (dashed line) than previously since macrodendrites project beyond the diffusion boundary layer.

Therefore, in view of these preliminary observations, it clearly comes out that the hydrodynamic conditions, the electric field, the time evolution and the pH value (through the hydrogen evolution reaction (HER)) are the governing factors and their action on the EHD impedance has been examined more carefully.

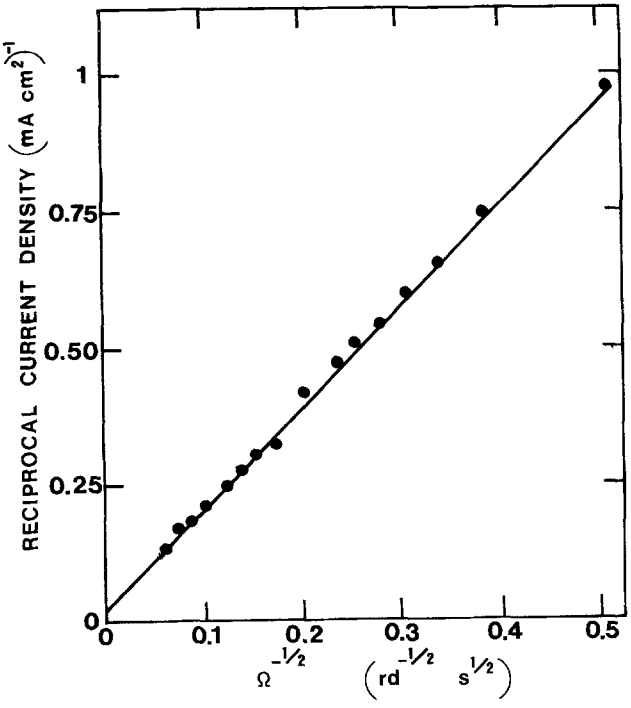

Fig. 2. Koutecky–Levich plot (I^{-1} vs $\Omega^{-1/2}$) at E = −0.7 V (SSE). Same conditions as Fig. 1.

3.2. *EHD impedance*

In this technique, the angular velocity of the disk electrode is modulated with time t around a mid value $\bar{\Omega}$ such that the instantaneous value is defined as:

$$\Omega(t) = \bar{\Omega}(1 + \varepsilon \cos \omega t)$$

where $\varepsilon \leqslant 0.1$ so as to keep within the linearity domain [3, 4]. ($\omega/2\pi$ is the modulation frequency (Hz).)

3.2.1. Influence of the mean angular velocity $\bar{\Omega}$. The EHD impedance diagrams were recorded for each average angular velocity with a freshly polished electrode. A complete diagram was then obtained within 20 min after immersion of the electrode. Measurements were performed at constant potential (−0.7 V (SSE)) at the beginning of or just below the diffusion plateau. According to the theoretical requirements, the EHD impedance for a system under complete mass transport control with infinitely fast interfacial kinetics and a uniformly reactive interface can be expressed as a function of one dimensionless frequency $pSc^{1/3}$ where $p = \omega/\bar{\Omega}$ and the Schmidt number Sc is the ratio of the kinematic viscoscity ν to the molecular diffusion coefficient D of the diffusing species. So, for a given system (and therefore for a given Sc value), the experimental 'reducibility' of the

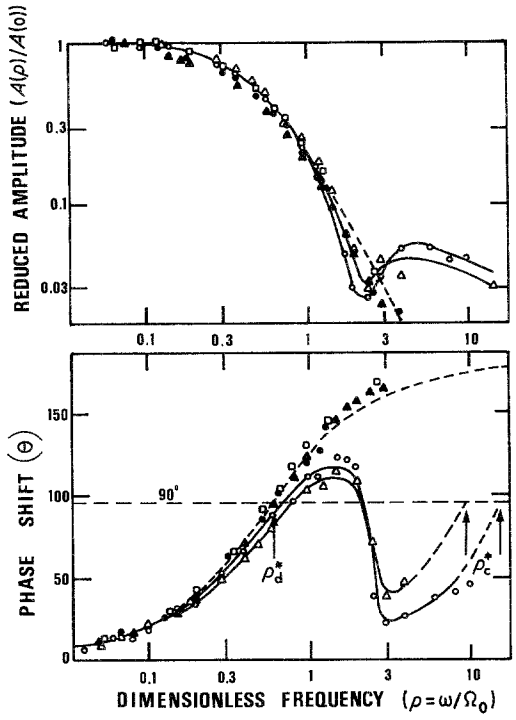

Fig. 3. Electrohydrodynamical diagrams in Bodes coordinates at $E = -0.7$ V (SSE) and for different mean angular velocities. (○) 60; (△) 120; (▲) 600; (□) 900; (●) 1200 rpm. The theoretical EHD impedance on a uniform accessible electrode calculated for $Sc = 125$ is represented by the dotted lines.

data vs p must be checked as $\bar{\Omega}$ is varied in a wide range.

The EHD diagrams presented in Fig. 3 in Bode coordinates (reduced amplitude $A(p)/A(0)$ and phase shift θ vs p) reveal two limiting behaviours according to the $\bar{\Omega}$ value:

(i) At higher values ($\bar{\Omega} = 600$, 900, 1200 rpm), the data fall on a single dashed curve corresponding to a fitted Schmidt number of 125. This unusually low value results from the high temperature. The system can then be considered as ideal, i.e. the interface is uniformly accessible from the view point of mass transport. This result is confirmed by the morphological aspect of the interface depicted in the Fig. 4a, characterized by a regular and short cut 'lawn' where the elementary structures have lateral dimensions of about 50 nm. No larger scale structures appear.

From these data, the molecular diffusion coefficient of $HTeO_2^+$, taking into account a kinematic viscosity of $0.33 \times 10^{-2}\,cm^2\,s^{-1}$, was calculated as:

$$D = 2.6 \times 10^{-5}\,cm^2\,s^{-1}$$

This value can be used as a reference in the studies of CdTe electrodeposition. Returning to the d.c. measurements, it is possible to deduce the solubility of $HTeO_2^+$. In fact, the Levich relation, improved by the Schmidt number correction [12], allows calculation of C_s:

$$i = \frac{0.62nFC_sD^{2/3}\nu^{-1/6}\Omega^{1/2}\pi R^2}{1 + 0.298Sc^{-1/3}} \qquad (1)$$

The result is $C_s = 9.2 \times 10^{-4}\,mol\,l^{-1}$ which gives a more accurate value than that previously estimated [7].

(ii) At lower values ($\bar{\Omega} = 60$, 120 rpm): the phase shifts and amplitudes follow the theoretical disk response only in the low frequency domain (i.e. for $p < 1$). At higher frequencies, a significant divergence is observed, the properties of this new behaviour being very similar to those of a partial blocking of the interface [6]. This topography gives a relatively satisfying reducibility of the diagrams in the HF regime as well, as predicted in Ref. [6]. Indeed, the HF behaviour may be ascribed to the summed contributions of the individual active sites, which are reducible vs p, and the site dimensions, d, can be deduced from the frequency difference between the two characteristic frequencies of the HF and the LF regimes.

According to [6]:

$$d = 2.1^{3/2}R(p^*_{HF}/p^*_{LF})^{-3/2} \qquad (2)$$

The deposit aspect in these conditions (Fig. 4b) shows the same microstructures as those of Fig. 4a. However, in addition, macrostructures with a 'bush-like' shape have now emerged and provide an average characteristic dimension estimated as about 40 μm.

The order of magnitude of p^*_{HF}/p^*_{LF} deduced from Fig. 3 is about 40 and therefore an average dimension

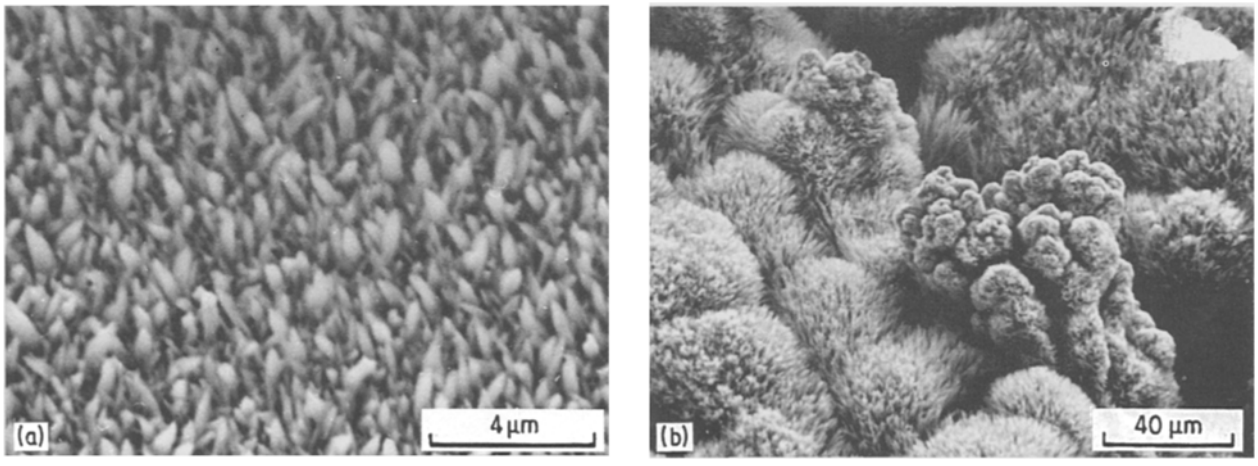

Fig. 4. SEM micrographs of tellurium electrodeposited at different rotation rates. (a) $\bar{\Omega} = 1200$ rpm; $E = -0.7$ V (SSE); (b) $\bar{\Omega} = 64$ rpm; $E = -0.675$ V (SSE).

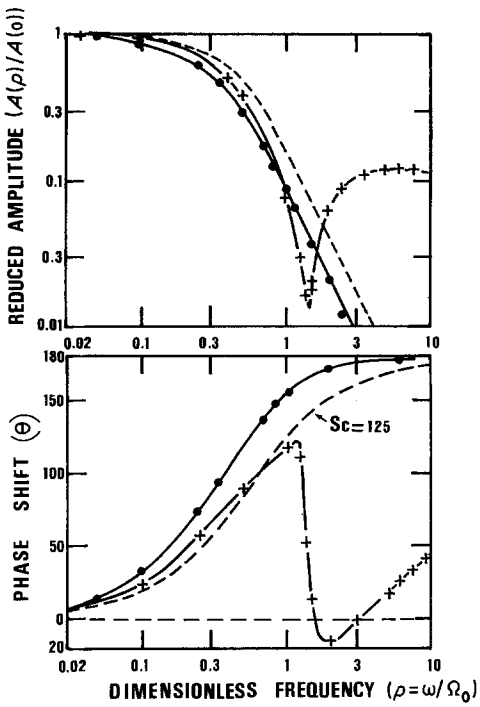

Fig. 5. EHD impedance diagrams for two potentials. $\bar{\Omega}$ = 120 rpm; (●) E = −0.55 V (SSE); (x) E = −0.7 V (SSE).

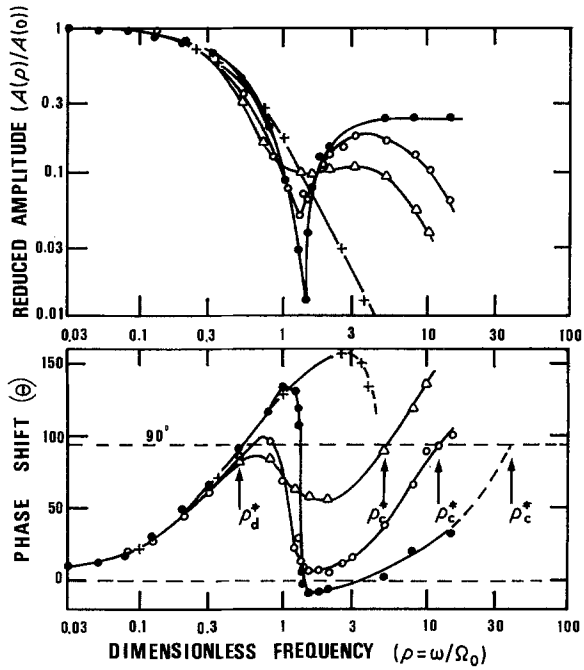

Fig. 7. EHD impedance diagrams for different hold times: (+) 15 min; (●) 25 min; (○) 40 min; (△) 2.5 h. $\bar{\Omega}$ = 120 rpm; E = −0.7 V (SSE).

of the active sites of 70 μm by use of Equation 2 can be estimated.

Two additional partial conclusions can be drawn from these first results. (i) Hydrodynamic conditions are able to induce macrostructures but do not strongly influence the sublying microstructures; (ii) the evolution of the diagrams with $\bar{\Omega}$ allows one to exclude a limitation of Te electrodeposition kinetics by the decomplexation reaction of $HTeO_2^+$. In fact, this should lead to a different set of EHD diagrams with $\bar{\Omega}$ with, in particular, no reducibility vs p in the HF domain [13].

3.2.2. Influence of the overpotential. The relative control of the overall kinetics by mass transport or by charge transfer can be changed according to the potential applied to the electrode. In particular, below the limiting diffusion plateau, the decreased control by mass transport is known to inhibit the formation of dendrites [14, 15].

In Fig. 5, the diagrams plotted at two potentials (with $\bar{\Omega}$ = 120 rpm), one at −0.7 V (SSE) (i.e. on the diffusion plateau), the other at −0.55 V (SSE), illustrate this conclusion. The one at −0.7 V (SSE) is similar to that already presented in Fig. 3 and is explained by the existence of macrostructures visible in Fig. 4b. At −0.55 V (SSE), the diagram shows no blocking effect and, for example, the phase shift has a limiting value of 180° as predicted by the theory [3, 4]. Accordingly, the micrograph taken in these conditions (Fig. 6) is very similar to Fig. 4a, i.e. with no evidence of macrostructures. However, the experimental EHD data do not coincide with the theoretical diagram at Sc = 125 previously found on the diffusion plateau. This effect is due to a contribution of the faradaic impedance, Z, and of the diffusion impedance, Z_D, which have different values in the frequency range

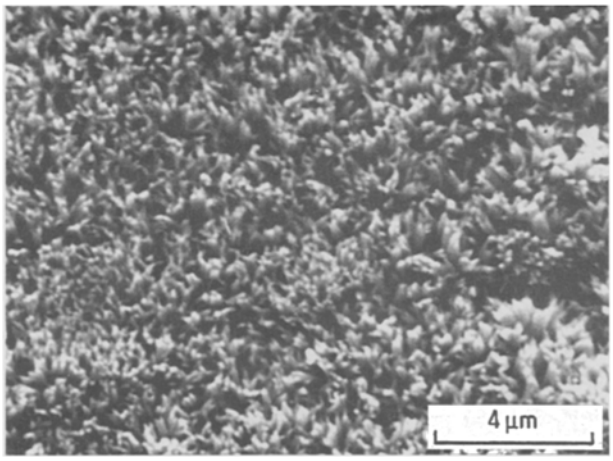

Fig. 6. Morphology of tellurium deposits prepared in mixed kinetics conditions. E = −0.55 V (SSE); $\bar{\Omega}$ = 120 rpm; hold time 25 min.

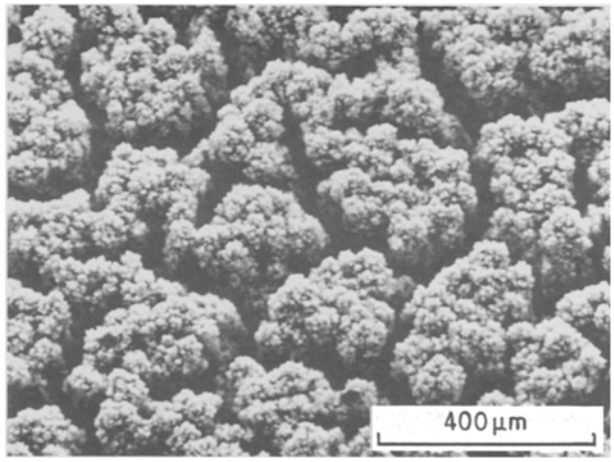

Fig. 8. Spatial distribution of a thick tellurium deposit. E = −0.7 V (SSE): $\bar{\Omega}$ = 120 rpm; hold time: 2.5 h.

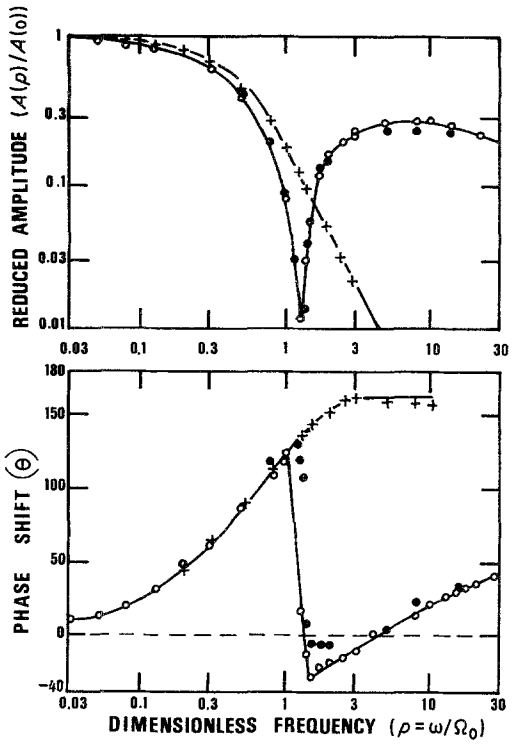

Fig. 9. EHD impedance diagrams for different pH values: (○) 2.1; (●) 2.2; (+) 3.

investigated. This deviation with respect to the case of the diffusion plateau has been calculated [3, 4] and the potentiostatic EHD impedance $(Z_{EHD})_p$ takes the following form by neglecting the influence of the double layer capacitance:

$$(Z_{EHD})_p = nFD\frac{Z_D Z_C}{Z}$$

$nFDZ_C$ is the quantity measured on the plateau.

3.2.3. Influence of the hold time (Fig. 7). When the time of deposition is increased, the following facts are observed: the LF regime remains identical; the HF regime takes place at lower p values as the elapsed time is increased; the transition between the LF and HF regimes becomes smoother with elapsed time.

At the shorter time investigated ($t \leqslant 15$ min), the experimental EHD diagram follows the theoretical one corresponding to a uniformly accessible surface and proves the absence of any blocking effect. This latter one appears after 25 min. The dimensions of active zones, evaluated by using Equation 2, are 15 μm (25 min), 170 μm (40 min) and 500 μm (2.5 h) and seem to be correlated, not to the size of the microstructures, but to the size of the bushes as seen in Fig. 4b or Fig. 8.

As a comparison, the SEM micrograph of Fig. 8, taken after 2.5 h, shows a completely different structure than that of Fig. 4b, and is characterized by a 'cauliflower'-like aspect. Some consistency can then be found between these structures with dimensions of about 400 μm and the dimension of 500 μm provided by the EHD data.

The smoothness of the transition in this latter case, compared with the sharp one at shorter times, indicates, in agreement with the theory, an increase of the inactive portions of the electrode area represented here by the 'canyons' between the big clusters.

3.2.4. Influence of the pH. The pH is a crucial parameter for several reasons: (i) the solubility of $HTeO_2^+$ is nearly proportional to $[H^+]$ according to [7]; (ii) the potential at which the HER becomes significant depends on the pH; (iii) H^+ is directly involved in the overall electrodeposition reaction:

$$HTeO_2^+ + 3H^+ + 4e^- \rightleftharpoons 2H_2O + Te\downarrow$$

In fact, this reaction may be split into several chemical (decomplexation) and electrochemical elementary reactions.

In Fig. 9 are plotted the diagrams for pH = 2.1 and 3 at $E = -0.7$ V (SSE) and $\bar{\Omega} = 120$ rpm. For pH = 2.1 the diagram is very close to the previous one obtained in similar conditions for pH 2.2 and proves the satisfying repeatability of the measurements. However, the microdendrites are much thinner than for pH = 2.2 (Fig. 4b) and therefore the bushes collapsed during the drying process preceding the introduction of the sample to the microscope, giving SEM images such as in Fig. 10a.

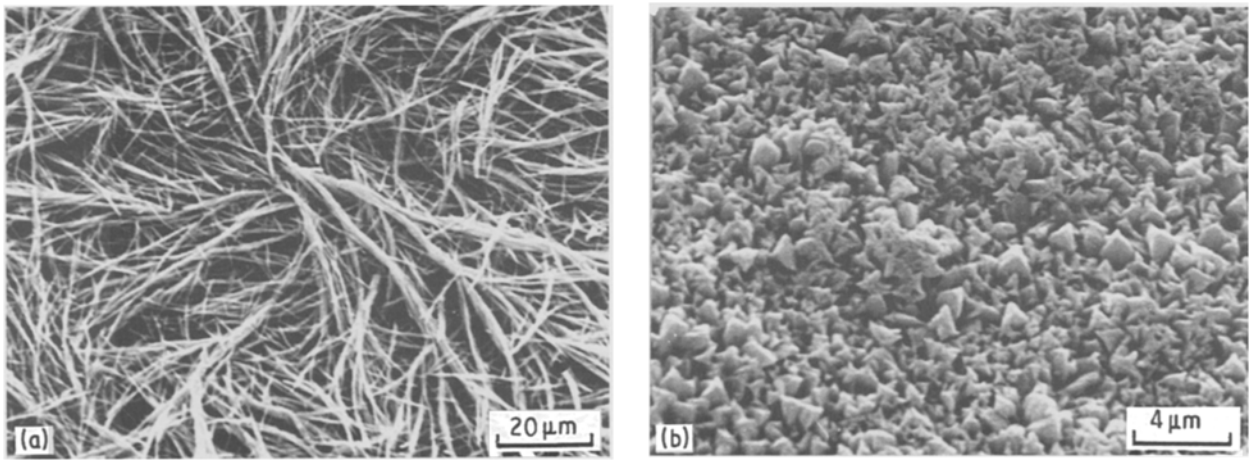

Fig. 10. Effect of the pH on the growth morphology of tellurium deposits. $E = -0.7$ V (SSE); $\bar{\Omega} = 120$ rpm. (a) pH = 2.1; (b) pH = 3.

The diagram recorded at pH = 3 follows the theoretical one corresponding to $Sc = 125$ very well, and shows no evidence of partial blocking. SEM observations (Fig. 10b) corroborate this conclusion since only microstructures are visible.

4. Discussion and conclusion

The set of results presented here provides a good example of the links existing between the interfacial kinetic properties of an electrochemical system and the morphological aspect of the interface which reflects the effect of the inhomogeneous reactivity of the substrate integrated over a certain period of time. The orders of magnitude of the growth figure dimensions deduced from both approaches were quite similar, though a detailed description of the morphology from the impedance data is still not possible. In fact, some limitations must be underlined.

(i) The analysis of interface heterogeneities by the EHD impedance is limited to dimensions above about 1 μm [16] because convective diffusion is not the mass transport prevailing process at this length scale. As a consequence, it is not possible to correlate the formation of the microstructures visible on Figs 4a, 6 or 10b, and spherical diffusion which is expected for such dimensions.

(ii) The model developed in Ref. [6] was established for a well-defined geometry with only one characteristic dimension whereas the tellurium electrodeposits reveal some size distribution.

(ii) Finally, another approximation was made in this work by applying a two-dimensional model to a three-dimensional system: this may be justified to a certain extent from the estimated values of the Nernst diffusion layer

$$\delta_N = 1.61 D^{1/3} \Omega^{-1/2} \nu^{1/6}$$

Due to the high D value calculated previously δ_N decrease from 80 to 20 μm when Ω varies from 6 to 100 rd s^{-1}, within the velocity domain investigated. Except for the longer hold times, the characteristic dimensions of the structures are smaller than the average thickness of the diffusion layer. In this situation, when mass transport is the rate determining step, dendritic growth is expected [14, 15]. On the contrary, when the process associated with interfacial kinetics (e.g. insertion of metallic ions in a crystal) is slowed down, then a more compact deposit is obtained.

The relative importance of both effects was recently demonstrated in work by Voss and Tomkiewicz [17] who simulated, by a Monte Carlo technique, the diffusion process for a particle, followed by its aggregation in a solid wall, the rate of which was represented by a sticking coefficient. In our case, the electron transfer rate of electrodeposition is the equivalent of the sticking coefficient. For a mass transport-controlled system with a strong sticking coefficient one expects a dendritic growth with a fractal geometry. Such a morphology is obtained with tellurium electrodeposition on the diffusion plateau where electron transfer rate is high. In contrast, a low sticking coefficient (analogous to a low overpotential) leads to smooth deposits as shown in Fig. 6.

Among different parameters investigated, hydrogen has been demonstrated to play a major role in the deposit structure. This fact is known for many metals, as for example, nickel [18]. At pH 2 or 3, it has been shown by EHD impedance that the decomplexation step of tellurium is not the rate determining one as usual for many systems. At pH 2, the higher H^+ concentration shifts the commencement of HER towards positive potentials: possible microbubble formation would then induce some heterogeneity in the deposit growth which may affect the EHD response. At pH 3 and for the same potential, this effect is, therefore, anticipated to be smaller.

In conclusion, it has been shown that tellurium electrodeposition proceeds under purely diffusional control in the region of the cathodic plateau and that the decomplexation reaction of $HTeO_2^+$ is not rate determining. Experimental conditions were defined such that the diffusivity of $HTeO_2^+$ could be accurately determined by use of the EHD impedance method and hence a better value for the solubility of this species was given. However, this work shows that the most attractive advantage of the EHD impedance method is that a fast and *in situ* diagnosis of the presence of a macroscale heterogeneity is provided, in agreement with the direct SEM observation. This fact ultimately justifies the principle of applying to a three-dimensional real system the concepts developed for a two-dimensional model and should be useful for many electrocrystallization problems.

References

[1] C. Sela, P. Boncorps and J. Vedel, *J. Electrochem. Soc.* **133** (1986) 10, 2043.
[2] P. Boncorps, Thèse Paris VI (1987).
[3] B. Tribollet and J. Newman, *J.E.C.S.* **130** (1983) 2016.
[4] C. Deslouis and B. Tribollet, 2e forum sur les Impédances Electrochimiques, Montrouge (1987) pp. 3–43.
[5] C. Sella, Thèse de 3e Cycle, Paris (1985).
[6] A. Caprani, C. Deslouis, S. Robin and B. Tribollet, *J. Electroanal. Chem.* **238** (1987) 67.
[7] L. E. Lyons, G. C. Morris, D. H. Horton and J. Keyes, *J. Electroanal. Chem.* **168** (1984) 101.
[8] C. Deslouis, G. Gabrielli and B. Tribollet, 168th ECS Meeting, New Orleans (USA), Oct. 1984.
[9] C. Deslouis, B. Tribollet, M. Duprat and F. Moran, *J.E.C.S.* **134** (1987) 2496.
[10] G. Maurin, O. Solorza and H. Takenouti, *J. Electroanal. Chem.* **202** (1986) 327.
[11] C. Deslouis, G. Maurin, D. Pottier and B. Tribollet, 38th ISE Meeting, Maastricht, Sept. 1987.
[12] J. Newman, *J. Phys. Chem.* **70** (1966) 1327.
[13] C. Deslouis and B. Tribollet, Journées d'Electrochimie, Dijon (France), Juin 1987.
[14] N. Ibl, *Oberfl. Surf.* **1b** (1975) 23.
[15] A. R. Despic and K. I. Popov, in 'Modern Aspect of Electrochemistry', Plenum Press, New York (1972) Vol. 7, p. 199.
[16] A. Ambari, C. Deslouis and B. Tribollet, *I.J.H.M.T.* **29** (1986) 35.
[17] R. F. Voss and M. Tomkiewicz, *J.E.C.S.* **132** (1985) 371.
[18] J. Amblard, M. Froment and N. Spyrellis, *Surf. Technol.* **5** (1977) 205.